

FRACTURE PROPERTIES OF POLYAMIDE 6/CLAY NANOCOMPOSITES

Bui Chuong and Tran Hai Ninh

Polymer Center, Hanoi University of Technology, Vietnam

BẢN TÓM TẮT

Tên bài báo : ĐẶC TRƯNG PHÁ HUỖ CỦA VẬT LIỆU POLYAMIT 6/CLAY NANOCOMPOZIT

Tên tác giả : BÙI CHƯƠNG
TRẦN HẢI NINH e-mail: ninhth-pc@mail.hut.edu.vn

Đơn vị công tác: TRUNG TÂM NGHIÊN CỨU VẬT LIỆU POLYME –
TRƯỜNG ĐẠI HỌC BÁCH KHOA HÀ NỘI

Địa chỉ : Tầng 2- C10 - Trường Đại học Bách Khoa Hà nội - số 1-Đại Cồ Việt
– Quận Hai Bà Trưng – Hà nội

Vật liệu Polyamid 6/clay nanocompozit được chế tạo bằng phương pháp trộn nóng chảy trên máy trộn kín Brabender. Cấu trúc nanno được xác định bằng phương pháp nhiễu xạ tia Ronghen (XRD) và ảnh hưởng của hàm lượng nanoclay đến tính chất cơ học của vật liệu được đánh qua các thông số: độ bền kéo, modun kéo, độ dẫn dài khi đứt và độ bền va đập. Kết quả nhiễu xạ tia Ronghen chỉ ra rằng cấu trúc nano tróc lớp được hình thành với hàm lượng nanoclay tương đối nhỏ (khoảng < 4 PTL), cấu trúc nano dẫn lớp và cấu trúc compozit vi mô xuất hiện khi hàm lượng nanoclay tăng lên. Sự xuất hiện các cấu trúc nano trong vật liệu khi hàm lượng clay tăng lên đã ảnh hưởng lớn đến tính chất cơ học của vật liệu: độ bền kéo tăng rất nhanh với hàm lượng clay nhỏ, đạt giá trị cực đại và giảm dần (tăng từ 60MPa đối với PA6 đến 86MPa của PA6 chứa 4PTL nanoclay – tăng 43%); modun cũng tăng lên khi hàm lượng clay tăng; trong khi độ dẫn dài khi đứt và độ bền va đập giảm rất nhanh khi có mặt nanoclay. Độ bền dai phá huỷ, G_{IC} , của vật liệu được xác định bằng phương pháp cơ học phá huỷ đàn hồi tuyến tính. G_{IC} giảm khi hàm lượng clay tăng chứng tỏ sự tương tác giữa lớp nanoclay và mạch polyme làm giảm sự linh động của mạch polyme. Điều này cũng được thể hiện qua sự thay đổi hình thái học bề mặt phá huỷ mẫu quan sát bằng kính hiển vi điện tử quét (SEM).

FRACTURE PROPERTIES OF POLYAMIDE 6/CLAY NANOCOMPOSITES

Bui Chuong and Tran Hai Ninh

Polymer Center, Hanoi University of Technology, Vietnam

ABSTRACT

Polyamide 6/clay nanocomposites were prepared via direct melt compounding using a conventional Brabender mixer. The influence of the clay content on the mechanical properties of the nanocomposites has been investigated. The XRD results indicated that the nanoclay were intercalated and partly exfoliated in the PA6 matrix. Mechanical test showed that the tensile modulus, yield strength increased steadily while the elongation at break decreased with an increase in the nanoclay content. The toughness of compounded materials was characterized using linear elastic fracture mechanics approach. The critical energy release rate, G_{IC} , decreased as the clay loading increased. The morphology of the fracture surfaces were investigated by SEM. The reduction in ductility and toughness was attributed to the constrained mobility of polymer chains in the presence of nanoclay particles.

1. INTRODUCTION

Nanocomposites refer to composites where one of the components has at least one dimension of the order of a few nanometers. They are a relatively new class of materials. One of the most promising composite systems would be hybrids based on organic polymers and inorganic clay minerals consisting of layered structure. Compared to their micro- and macro counterparts and the net polymer matrix, polymer/clay nanocomposites (PCN) exhibit improved tensile strength and module, decrease gas permeability, thermal expansion, flammability [1-6]. The enhanced properties of PNC are presumably due to the formed nanoscale structure, the large aspect ratio and large area of the layered silicates, and strong interaction between polymer molecular chains and layered silicates.

PCN has been prepared in three different ways: solution interaction, in-situ polymerization, and direct melt intercalation [2]. The first two methods are limited because neither a suitable monomer nor a compatible polymer-clay solvent system is always available. Moreover, they are not always compatible with current polymer processing techniques. Among all the methods to prepare

PCN, the approach based on direct melt intercalation perhaps the most commercial and environmentally-friendly impact.

Polyamide 6 (PA6) is a kind of important engineering plastic. There are a lot researches on PA6/clay nanocomposites in many aspects, such as effect of different types of clay [7], the condition of melt - intercalation process [8], effect of molecular weight of PA6 [9], crystallization, structure of nanocomposites and so on.

In this article, we focus on the mechanical and fracture properties of PA6/clay nanocomposites and we describe how the mechanical properties and fracture behavior of materials depend on presence of clay.

2. EXPERIMENTS

2.1 Materials

Organically modified montmorillonite, (Nanomer[®] I28E onium ion montmorillonite was modified with octadecylamine), was provided by the Nanocor Inc. (USA), with a particles size of 8 - 10 μ m, and interlayer spacing of 22.07 \AA .

The Polyamide 6 (PA6) used in the present work was produced by the UB Corp. (Taiwan), with the melt flow index of 10g/10minutes (at 260°C, 2.16 kg). Before using, PA6 was air-dried under vacuum at 80°C for 12h to eliminate the water absorbed during the industrial washing.

2.2 Preparation of the PA6/clay nanocomposites

PA6/clay nanocomposites were synthesized using the following procedure: different amount of organoclays 2, 4, 6, and 10 part per hundred parts of polymer resin (phr) were manually added slowly to melt-state PA6 in a Brabender mixer. The mixing temperature was 230°C and the rotor speed was 100 rpm. When all the materials were added into the mixing chamber, the material were further mixed for 10 minutes. After mixing, the compound was cut into small pieces. These PA6/clay nanocomposites were denoted PA6/clay-*n*, where *n* represents the amounts of clay in the composites (phr).

2.3 Mechanical properties

A vertical injection-molding machine RAY-RAW (Italy) was used for preparing the samples for mechanical tests. The injected-molding temperature and pressure were 240°C and 80psi, respectively. The tensile (ASTM-D638-02a, type IV) and impact bars (ASTM-D256) of pure PA6 and nanocomposites were prepared. Prior to the mechanical testing, both the tensile and impact bars were conditioned at the temperature of 25 and the relative humidity of 60 ± 5% for 40h. Five specimens of each sample were tested and the mean values and standard deviations were calculated.

The fracture toughness of the specimens were determined using deeply notched three-point bending (SEN-3PB) test specimens (16mm in width (W), 3.5mm in thickness (B), 80mm in length(L)) according to ISO 13586 standard. Precracks were made by inserting a fresh razor blade into the machined slot and the crack-to-width ratio, *a*/*W*, was limited to 0.45-0.55 in all tests.

2.4 X-ray diffraction (XRD)

The nanocomposite samples in form of film (with thickness of 1mm) for XRD measurement were pressed in metal molder at 230°C for 5 min and naturally cooled down to room temperature.

The nanomer characteristic of the obtained product can be verified by X-ray diffraction (XRD). XRD was performed at room temperature by a SIEMENS D5000, the X-ray beam was nickel-filtered CuK α_1 ($\lambda = 0.154$ nm) radiation operated at 40kV and 30mA; data were obtained from 1° to 40° (2θ) at a rate of 2°C/min.

2.5 Morphology study

SEM observations of the materials were performed on scanning electron microscopy (SEM: JEOL 6360LV). Fractographic examinations were conducted on the specimens obtained from the fracture toughness test. All specimens were coated with platinum in a JEOL JFC-1600 auto fine coater before SEM observation.

3. RESULTS AND CONCLUSIONS

3.1 Characterization of the Nanostructure

XRD patterns of the hybrids obtained are used to evaluate the dispersion effect of montmorillonite layers in the polymer matrix, or what kind of nanostructure can be achieved. Figure 1 shows the XRD patterns of both the organoclay and the PA6/clay hybrid with different weight fractions of organoclay. The PA6 nanocomposites compounding with 2phr organoclay is abbreviated as PA6/clay-2, similarly, the nanocomposites having 4, 10phr clay loading are abbreviated as PA6/clay-4, and PA6/clay-10, respectively. The XRD pattern of the organoclay shows two characteristic peak ($d_{001} = 22.07$ Å) at 3.75° of 2θ and ($d = 10.98$ Å) at 5.2° of 2θ corresponding to the modified clay and non-modified clay part in organoclay. The peak position of pristine organoclay at $2\theta = 3.75^\circ$ (22.07 Å) shifted to a smaller angle of $2\theta = 2.8^\circ$ (35.35 Å) when the PA6 was reinforced with 10phr of clay, indicating that the PA6

chains diffused into the clay galleries to increase the layer distance. Note that there is appearance of a broader peak at $2\theta = 5.2^\circ$ (10.98 Å) corresponding to clay agglomeration existing in nanocomposites. For PA6 containing a 2 and 4phr of nanoclay content,

there existed inapparent and small peaks in the XRD results. The absence of a sharp (001) peak indicates that organoclay has a nearly exfoliated effect in the PA6 matrix. Clearly, the dispersion is better at lower clay loading than at a high clay loading.

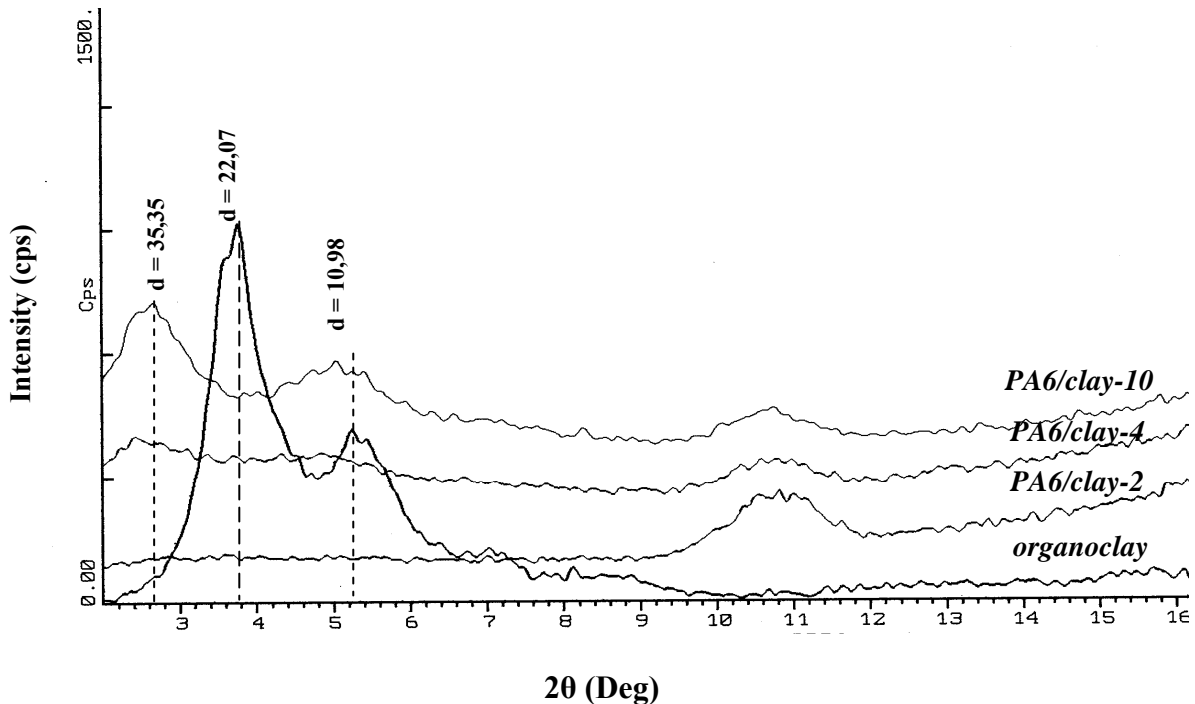


Figure 1: XRD patterns of PA6/clay with different organoclay contents.

3.2 Mechanical properties

Figure 2 shows the effect of clay concentration on the mechanical properties of PA6/clay nanocomposites. The tensile strength increases rapidly with increasing clay content from 0 to about 5phr, approaches the highest point of about 85MPa at 4phr, and declines slightly with further increment of the clay content. The tensile modulus increases sharply with the clay content in the range of 0-6phr, but changes little for clay content higher than 6phr.

The elongation at break for nanocomposite is greatly affected by the presence of clay. The elongation at break of 300% for neat PA6 drops dramatically to about 15% for nanocomposite containing only 2phr of clay. With an increase in clay content, the elongation at break declines slightly. The

similar phenomenon is observed in the dependence of Izod impact strength of PA6/clay on clay content as shown in Fig.2d. The notched impact strength remains constant at level of around 45J/m within the experimental error in the clay content range of 2-10phr.

The results indicate that PA6/clay has a dramatic increase in strength, modulus compared with PA6 pristine. The enhancing effect of organoclay on the stiffness and strength is probably due to the incorporation of clay platelets with PA6 matrix. The decrease observed with a clay loading above 6phr can be attributed to the presence of aggregation of the clay layers in high content. In addition, the decrease in elongation with clay concentration indicates that the resulting nanocomposites are very brittle.

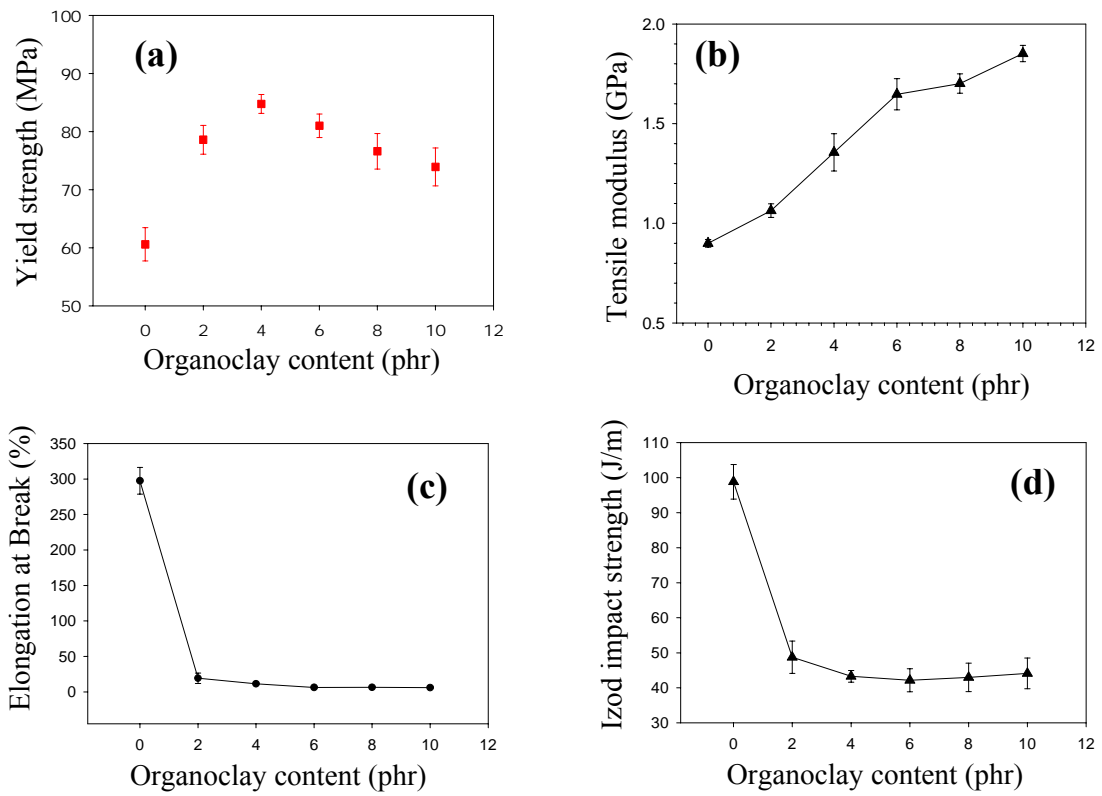


Figure 2 Mechanical properties of melt blending PA6/clay nanocomposites as a function of organoclay content: (a) yield strength, (b) modulus, (c) elongation at break, (d) Izod impact strength

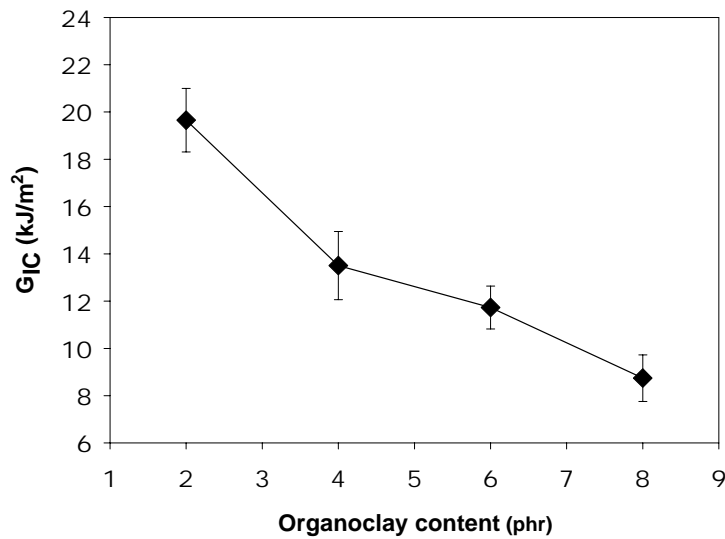


Figure 3 G_{IC} of PA6/clay nanocomposites versus clay content. The G_{IC} of unfilled PA6 does not satisfy the thickness conditions for plane-strain toughness

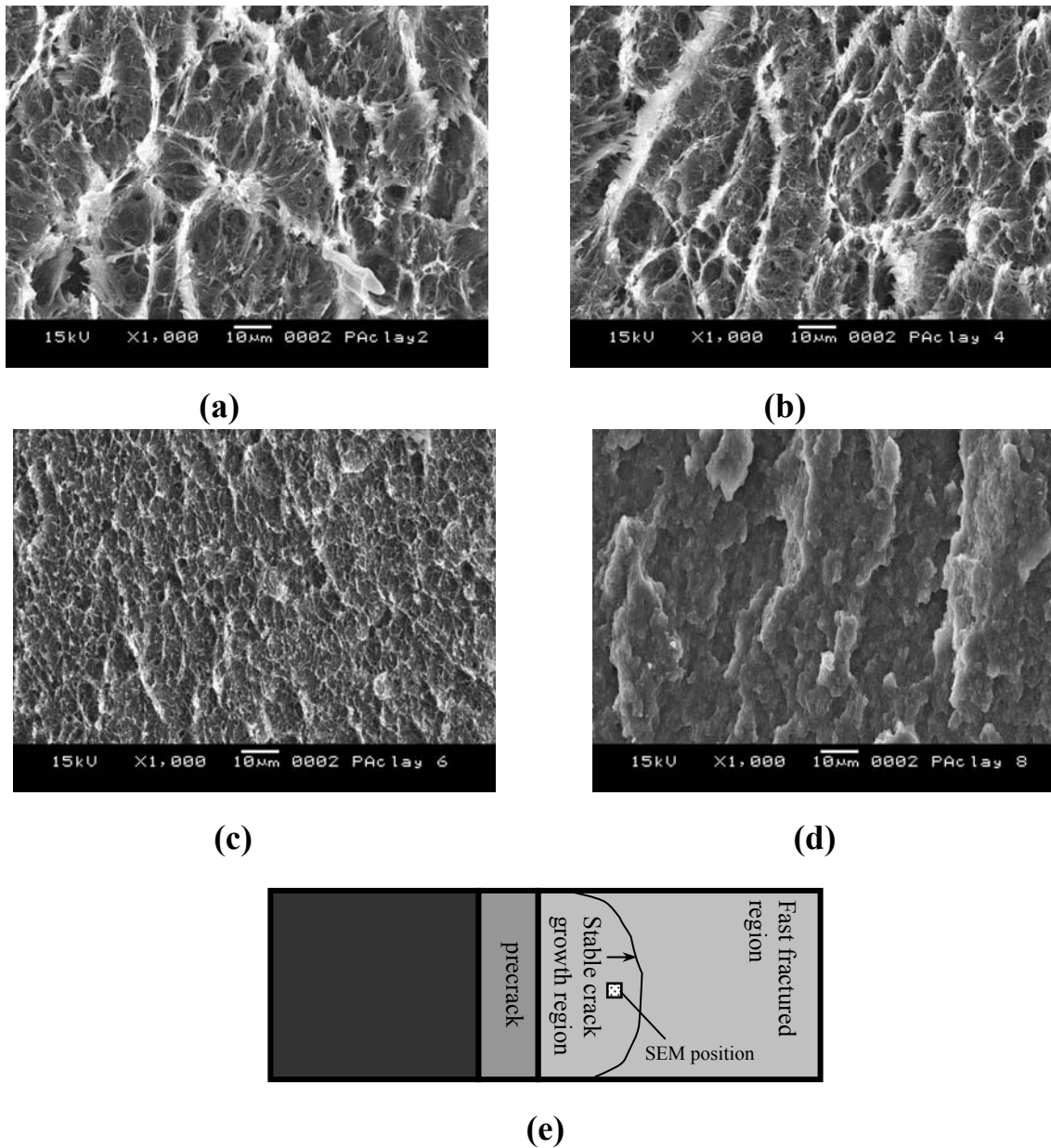


Figure 4 SEM photomicrographs of PA6/clay nanocomposites containing (a) 2phr, (b) 4phr, (c) 6phr, and (d) 8phr organoclay. (e) gives a schematic sampling position of the fracture surface under SEM observation. The arrow indicates the direction of crack propagation.

3.3 Fracture behavior

This study focused on the fracture properties of organoclay -filled PA6. Because the size of the layered clay is comparatively smaller than other inorganic fillers such as short glass fiber and the characteristic property of PA6/clay nanocomposites is rigid and brittle, we attempted using the linear elastic fracture mechanics (LEFM) approach to determine the

fracture toughness, G_{IC} , which is called the critical energy release rate. The fracture toughness was determined using three-point-bending (SENB) test specimen according to standard ISO 13586.

Figure 3 plots the fracture toughness, G_{IC} , versus the clay content. The fracture toughness value of pristine PA6 was not shown because the size requirement for valid value

could not satisfy the plane strain conditions. Figure 3 shows that the fracture toughness decreases steadily with an increase in clay loading. The trend in toughness appears opposite to that of the increase in strength and stiffness.

The locus of failure was microscopically examined. Figure 4 shows SEM micrographs of the fracture surface at the stable crack growth region for a series of typical specimens subjected to SENB condition. Figure 4(a-d) shows a transition from ductile to brittle fracture. The fracture surface of PA6/clay-2 [Fig.4 (a)] shows rather ductile features with extensive voiding and PA6 fibrous structures stretching over the crack face prior to fracture. With an increase of clay loading up to 6phr, the fibrils appear much finer and fracture surfaces are less rugged. Matrix deformation is greatly reduced when the clay loading is increased up to 8phr. The fracture surface becomes featureless and no fibril sites can be observed. The observation suggests that the presence of clay markedly hindered void formation during deformation and less PA6 chains were available for bridging the crack face. Clearly, fracture behavior changes from a rather ductile matrix voiding and fibrous deformation to featureless brittle cleavage when clay loading increase. The fracture toughness results in SENB tests are consistent with the change in elongation at break and impact strength.

4 CONCLUSION

PA6 was blended with organoclay using mixer method. The gallery spacing was shown to enlarge during melt compounding. The XRD results indicated that the organoclay was intercalated and exfoliated better at lower clay loading than at a high clay loading. Strength and stiffness increased greatly with an increase in the clay content, in general, but the fracture deformation showed a transition from ductile to brittle fracture. This high reinforcement effect implies a strong interaction between the matrix and the clay interface that can be attributed to the nanoscale and uniform dispersion of the silicate layers in the PA6 matrix. The reduction in ductility and toughness was attributed to the constrained

mobility of polymer chains in the presence of nanoclay particles. SEM photomicrographs were consistent in showing ductile voiding and fibrous structures and featureless cleavage at relative low and high loadings of clay, respectively.

Reference

1. Peter C. LeBron, et al. Polymer-layer silicate nanocomposites: an overview. *Appl. Clay. Sci.*, Vol. 19 (1999), p.11-29.
2. Suprakas Sinha Ray, Masami Okamoto. Polymer/layer silicate nanocomposites: a review from preparation to processing. *Progress in Polymer Science*, Vol.28 (2003), p.1539-1641.
3. J.W. Cho, D.R. Paul. Nylon 6 nanocomposites by melt compounding. *Polymer*, Vol.41, (2001), p.1083-1094.
4. Limin Liu, Zongneng Qui, Xiaoguang Zhu. Studies on Nylon6/Clay nanocomposites by melt-intercalation Process. *J. Appl. Polym. Sci.*, Vol. 71, (1999), p.1133-1138.
5. K.Masenelli, et al. Mechanical properties of clay reinforced Polyamide. *J. Appl. Polym. Sci.: Part B: Polym. Phys.*, Vol.40, (2002), p. 272-283.
6. T.D. Fornes, D.L. Hunter, D.R. Paul. Effect of sodium montmorillonite source on the nylon 6/clay nanocomposites. *Polymer*, Vol.43, (2004), p.2321-2329.
7. H.R. Denis, D.R. Paul, et al. Effect of melt processing condition on the extent of exfoliation in organoclay-based nanocomposites. *Polymer*, Vol.42, (2001), p.9513-9652.
8. T.D. Fornes, D.R.Paul. Nylon6 nanocomposites: the effect of matrix molecular weight. *Polymer*, Vol. 42, (2001), p.9929-9935.
9. E. Devaux, S. Bourbigot, A.E. Achari, Crystallization behavior of PA6 clay nanocomposites. *J. Appl. Polym. Sci.*, Vol.86, (2002), p.2416-2419.